SOME NEW ASPECTS OF POROUS SILICON

G. FISHMAN AND R. ROMESTAIN

Laboratoire de Spectrométrie Physique, Université Joseph Fourier-Grenoble I
and C.N.R.S.
B.P.87, 38402 Saint Martin d'Hères Cedex, France

We recall the geometry of porous silicon and the order of magnitude of some characteristic parameters. We give a brief review of optical experiments and their different interpretations. We focus on quantitative interpretations and show that an essential concept is confinement in a quantum wire or box. In particular, the exchange energy of electron–hole pairs correlated by Coulomb interaction inside a quantum box explains results obtained between 4 K and room temperature. Nevertheless, the large shift of the main luminescence line for similar porous silicon but different electrolytes cannot be explained by quantum confinement alone and has to be accounted for by the difference between the dielectric constants inside and outside the porous silicon. A brief account of electroluminescence experiments is also given.
PACS numbers: 78.50.Ge, 78.55.Hx, 78.60.Fi

> L' éponge est certainement une version du labyrinthe.
> (The sponge is surely a version of the labyrinth.)
> P.G. de Gennes [1]

1. Introduction

Although porous silicon (PS) had been known for a long time [2], it was only in 1990 that L.T. Canham showed in a famous experiment [3] that PS emitted visible light, roughly at 1.7 eV (0.7 μm), although the forbidden gap of silicon is 1.1 eV (1.1 μm). This emission was interpreted as a manifestation of quantum confinement in a quantum wire or box (of the order of a few nanometers), which is consistent with the understanding of the growth of nanostructures [4]. After some controversies [5] it is now generally accepted that this interpretation is correct but it is almost the only fact that is well established [6]. In the following, after having recalled the structure and a theoretical description of PS (Sec. 2), we present some experiments which give information about the origin of visible luminescence: absorption coefficient (Sec. 3), luminescence (Sec. 4) and a brief account of the electroluminescence (Sec. 5). Section 6 is devoted to the conclusion.

2. What is porous silicon?

PS is usually prepared by dissolving electrochemically monocrystalline silicon in HF solutions. Pore structures are related to the dopant type, acid concentration, anode current density, ... [7, 8]. Roughly speaking, PS is a kind of sponge, which means the shape of the quantum wires or boxes is not well determined even for a given sample [9, 10]. A useful order of magnitude is that the surface area of PS is of the order of 600 m^2/cm^3. If the silicon substrate is p^+ type, a description of PS as a set of more or less oriented wires (perpendicular to the substrate surface) will be useful. If the substrate is p type, a description as an isotropic sponge is more appropriate: quantum dots are linked by thin wires (by thin we just mean diameters of wires are smaller than the diameter of dots); in other words PS can be visualized as small loosely connected crystallites. Nowadays, typical diameters may be of the order of 30 Å, with porosities of up to 85% (i.e., the volume fraction of silicon in volume is 15%). As a result the band gap is strongly increased [11, 12].
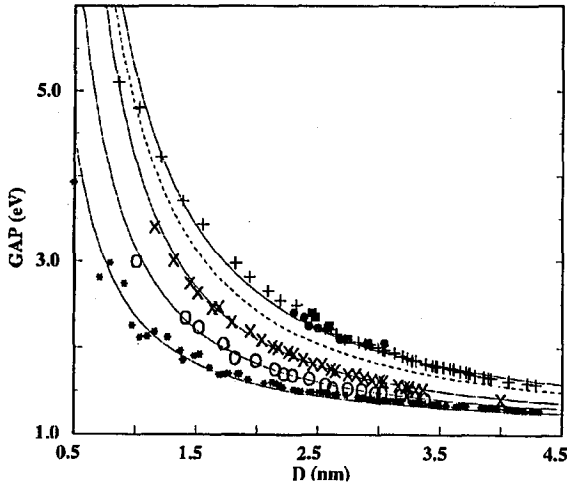

Fig. 1.   Calculated optical band-gap energies for various silicon crystallites (+) or wires (100 — ×; 110 — *; 111 — O) with respect to their diameter d. The continuous lines are an interpolation of these results using a d^{-n} law. The black dots and squares are experimental results. The dashed line is the band-gap energy for the crystallites including the Coulomb interaction between the electron and the hole. (After Ref. [11]).

Theoretical L.C.A.O. calculations give the band gap versus diameter L [11], see Fig. 1. The confinement energy is described by a $L^{-1.39}$ law. Another description was given in the effective mass framework [13]. The quantum well being finite, this leads to a $L^{-1.64}$ law (the effective mass in the quantum well is of the order of 0. 25 for the conduction band as well as for the valence band, while the barriers are of the order of 4 eV for both bands [14]).

3. Absorption

The transmission coefficient versus photon energy [15] was obtained for different porosities. From these results it is possible to deduce the absorption coefficient (Fig. 2), where the porosity is taken into account [16]. In other words the absorption corresponds to the quantity of matter in PS, which allows one to make a useful comparison with the absorption in bulk silicon. It is then possible to relate, at least qualitatively, the absorption to a PS mean size. The blue shift is a strong indication that the absorption is modified by quantum confinement; in itself, it does not prove that the luminescence is due to this confinement.
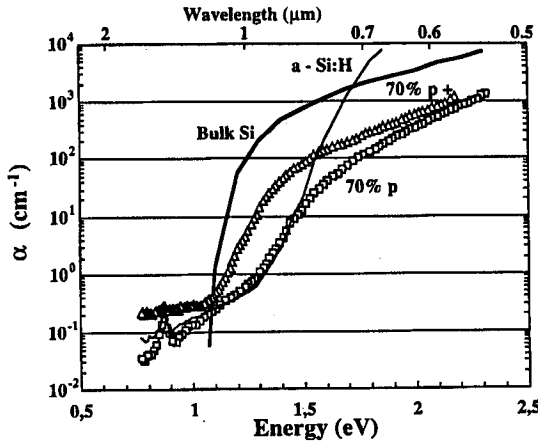

Fig. 2. Optical absorption coefficient versus photon energy for monocrystalline silicon, amorphous hydrogenated silicon, and p and p^+ 70% free-standing porous silicon. Reproduced with permission from Ref. [16]. Copyright by the Elsevier Science.

4. Luminescence

4.1. Luminescence lifetimes

The photoluminescence decay is not exponential, therefore it is useful to define an average lifetime $\tau = (1/I_{max}) \int I(t)dt$ [17], where $I(t)$ is the luminescence intensity and I_{max} the signal at the time $t = 0$. The photoluminescence decay rate $1/\tau$ is related to the radiative W_R and nonradiative rates W_{NR}, $1/\tau = W_R + W_{NR} \approx W_{NR}$. The decay rate is given in Fig. 3 as a function of photon energy and is described by the relation $W_{NR} \propto \exp(E/\beta)$, where $\beta = 0.28$ eV. This dependence upon confinement energy suggests two possibilities: a temperature-activated process or an escape by tunneling through barriers surrounding the confined zone. The first process is ruled out because β is more than ten times larger than kT at room temperature. The calculation of the variation of the tunneling rate with likely parameters leads to a barrier thickness of the order of 3 nm, which is in
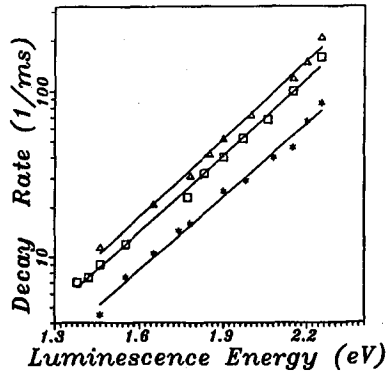
Fig. 3. Dependence of photoluminescence decay rates on photon energy for three 65% porosity layers that differ by oxidation level increasing from the top curve to the bottom one. Measurements were made at room temperature. (After Ref. [17]).

the range of sizes that characterizes the oxidized porous silicon structure. Via the usual density of states function of the energy $\rho(E)$ it is quite simple to relate the size distribution $\rho(L)$ to the density of states versus the wavelength: $\rho(L)\mathrm{d}L = \rho(E_{\mathrm{cv}})\mathrm{d}E_{\mathrm{cv}} = \rho(\lambda)\mathrm{d}\lambda$, where E_{cv} is the sum of the confinement energies (conduction and valence band) and $(E_{\mathrm{cv}} + E_{\mathrm{G}})\lambda = C = 1.24$ (eV μm); E_{G} is the band gap. Now the luminescence intensity is $I(\lambda) \propto \rho(\lambda)W_{\mathrm{R}}/(W_{\mathrm{R}} + W_{\mathrm{NR}})$; in a rough approximation W_{R} is independent of the energy [17] contrary to W_{NR} so that $I(\lambda) \propto \rho(\lambda)\exp(C/\beta\lambda)$. This relation between the luminescence and the statistical description of the model of spheres gives parameters of the order of 3 nm for the average diameter L_{m} and 0.5 nm for the root-mean-square σ. This description can be improved by taking into account the probability that a crystallite may have a non-radiative recombination centre on its surface and therefore does not luminesce [18] but this does not substantially change the above values.

What has just been described allows one to understand the origin of the linewidth [13] but does not describe the luminescence mechanism itself. This problem was tackled by P.D.J. Calcott and co-workers [19, 20], who showed that the luminescence is related to crystallites as shown in Fig. 4, where the replicas are related to momentum conserving phonons of bulk silicon: this is the best evidence for the Si indirect gap. They also showed that the origin of luminescence was due to radiative recombination of electron–hole pairs in crystallites as confirmed by another group [21]. In fact in small crystallites, i.e. for crystallites whose "radius" R is smaller than the average exciton Bohr radius a^* in bulk silicon (which is of the order of 40 Å [22]), there is no difference between an electron-hole pair and an exciton. This comes from the fact that for $R \ll a^*$ the kinetic energy proportional to $1/R^2$ is much higher than the (absolute value of the) electrostatic interaction potential which varies as $1/R$ [23]. Figure 5 shows the radiative lifetime of PS luminescence recorded at 1. 77 eV (0.7 μm). This behaviour was explained in Ref. [19] and confirmed by a more sophisticated calculation [23]. A two-level description of the excited state is used, the lower one being almost non-radiative (i.e. having a
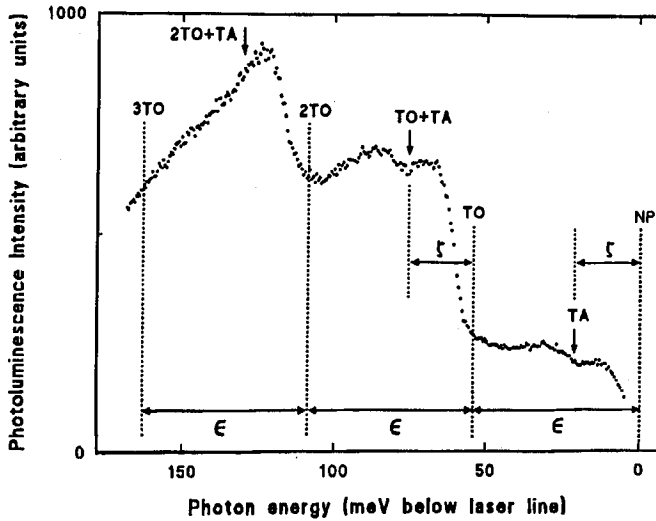
Fig. 4. Photoluminescence spectrum taken at 2K with resonant laser excitation at 1.611 eV and a mean power density of 3 W cm^{-2}. Reproduced with permission from Ref. [20]. Copyright by the Elsevier Science.
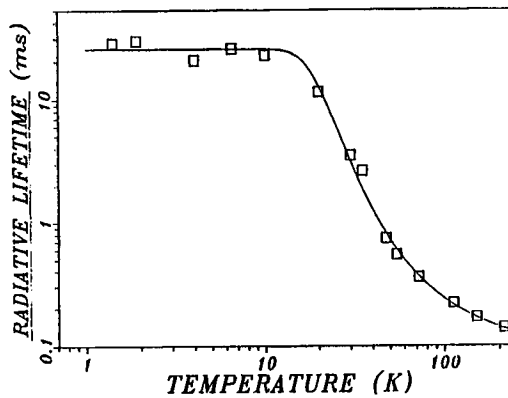

Fig. 5. Temperature dependence of radiative lifetime of the PS luminescence recorded at 1.77 eV. The solid line is the best fit of the experimental data with the following parameters: electron–hole exchange interaction = 10 meV, lifetime of the forbidden triplet (allowed singlet) level = 25 ms (22 microseconds). (After Ref. [21]).

long radiative lifetime) and the higher one being radiative (with a short radiative lifetime). This splitting is due to the electron–hole exchange interaction which is here of the order of 10 meV. In bulk silicon the electron–hole exchange interaction E_x is of the order of 0.15 meV [24] for the exciton. In a small crystallite, assumed to be spherical, it is easy to show that the exchange interaction is of the order of $2.1(a^*/R)^3 E_x$, where the numerical factor is a geometrical factor [21].

For $R \approx 13$ Å we find that the electron–hole exchange splitting is of the order of 10 meV. Here it is worth noting that two different experiments [19, 21] lead to the same interpretation with the same order of magnitude and no other explanation has been suggested up to now.

4.2. Luminescence spectra

However it has been noticed that a given PS may have different luminescence spectra and it is only recently that this puzzling problem has begun to have at least a beginning of solution. This is linked to the "environment" of the PS, which can be air (dry PS) or aqueous electrolyte (wet PS) [25]. The problem is not simple because intermediate situations, where PS is partly wet, may occur [26]. In principle, it would be possible to consider an exciton but the donor case is more easily tractable, so that we consider wires with infinite quantum barriers in the middle of which a donor (or an acceptor) is located. The key point is that the dielectric constant outside of wire has a strong influence on the whole electrostatic potential, even inside the wire [27]. The relevant parameter in this case is the ratio $\varepsilon = \varepsilon_e/\varepsilon_i$ of the dielectric constant of the embedding medium ε_e to the internal dielectric constant ε_i. Experimental results are given in Figs. 6 and 7, which show the correlation between infrared and luminescence experiments.
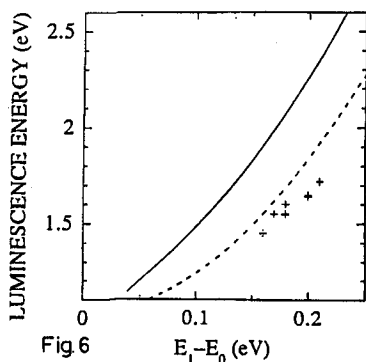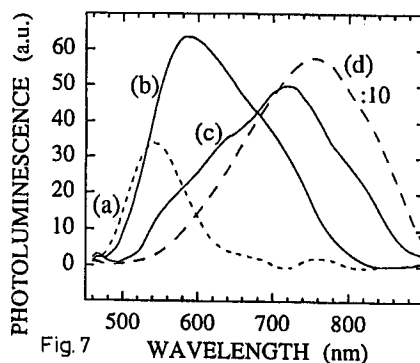

Fig. 6. Correlation between luminescence energy and ground-to-first-excited-state transition energy. The solid (dashed curve) corresponds to the band-to-band (impurity-to-band) luminescence. The bulk–Si is $E_G = 1.1$ eV and 0.1 eV is taken as the effective Hartree. Crosses: experiment. The energy $E_1 - E_0$ has been taken as the maximum of the observed photoinduced infrared absorption: see the text. Reproduced with permission from Ref. [25]. Copyright by the Éditions de Physique.

Fig. 7. Photoluminescence spectra of porous silicon aged in HF and transferred to various solvents: (a) in HF ($\varepsilon_{es} > 80$), (b) in 1,3 dioxolane ($\varepsilon_{es} \approx 6$), (c) in 1,4-dioxane ($\varepsilon_{es} = 2.2$), (d) in air. Excitation light: 365 nm, 100 μW/cm². A red shift of the green band is seen to accompany the decrease in the dielectric constant of the embedding medium. (After Ref. [26]).
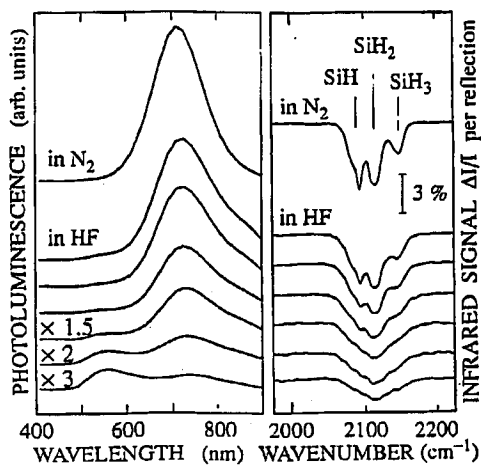
Fig. 8. Evolution of the photoluminescence spectrum (left) and of the SiH absorption spectrum (right) of a red luminescent porous silicon sample when reimmersed in HF. The first spectra (labelled "in N_2") are those recorded immadiately prior to sample reimmersion in HF. The infrared spectrum exhibits three distinct contributions, ascribed to surface SiH, SiH_2 and SiH_3 groups. The subsequent label spectra (labelled 'in HF") are recorded *in situ* during etching. Etching times are respectively for these spectra from the top to the bottom of 5, 10, 30, 40, 45, 65 minutes. When etching proceeds, the progressive broadening of the SiH band is indicative of a progressive wetting of the surface. This broadening coincides with the diminution of the red line in the photoluminescence spectrum, leaving only the green one when the surface is completely wet. (After Ref. [26]).

Lastly Fig. 8 displays the influence of wettting on the luminescence spectrum. The infrared absorption is used as a standard to measure the wetting which allows one to know the luminescence versus the wetting.

5. Electroluminescence

Although electroluminescence is not quantitatively understood it is difficult to overlook experiments that show that the electroluminescence is strongly related to photoluminescence, at least when electroluminescence is performed in aqueous solutions [28, 29]. Figure 9 shows an example of the link between them. Only one normalization coefficient has been introduced to adjust the photoluminescence intensity relative to the electroluminescence spectra. The photoluminescence curve is then the envelope of the set of electroluminescence curves obtained at different voltages. Other experiments [29] confirm this tendency.

6. Conclusion

In this paper we have shown that the main features of luminescence in porous silicon are identified. We have deliberately ignored all the possible explanations which have not been able to be quantified at least until now. Some of them deserve some attention. For instance the surface states may play a part in the description
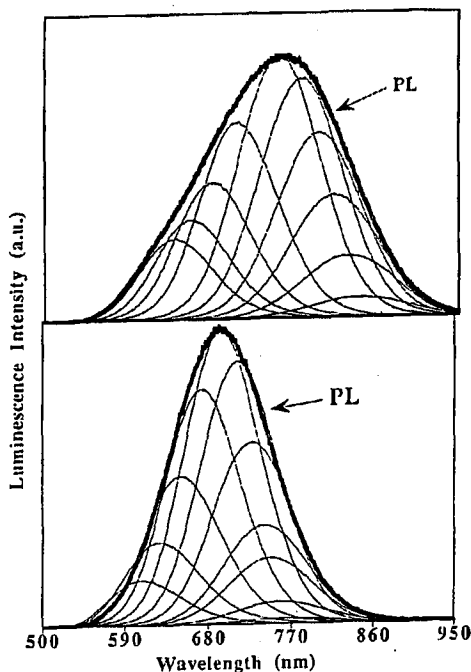
Fig. 9. The bold lines and the thin lines refer respectively to photoluminescence and electroluminescence spectra in two samples of different porosity. The corresponding electroluminescence spectra were recorded for a sequence of bias voltage with steps of 0.05 V. Only one curve of electroluminescence is normalized for one sample. (After Ref. [29]).

of the luminescence [30]; however, up to now no order of magnitude has been given, so that it is difficult to estimate the influence of the surface states. Wet electroluminescence is without any doubt related to luminescence but the detailed mechanisms still have to be clarified. Further studies are necessary to clear up at least this last point.

Acknowledgments

References

[1] P.G. de Gennes, Leçon inaugurale au Collège de France, Mercredi 10 novembre 1971 (Inaugural Lecture, Collège de France, Wednesday 10th November 1971).

[2] D.R. Turner, *J. Electrochem. Soc.* **105**, 402 (1958).

[3] L.T. Canham, *Appl. Phys. Lett.* **57**, 1046 (1990).

[4] V. Lehmann, U. Gösele, *Appl. Phys. Lett.* **58**, 856 (1991).

[5] *Proc. E.M.R.S. Spring Meeting, May 4-7, Strasbourg, 1993*, Eds. J.C. Vial, L.T. Canham, W. Lang, *J. Lumin.* **57**, 1–358 (1993).

[6] *Porous Silicon Science and Technology, Ecole des Houches*, Eds. J.C. Vial, J. Derrien, Springer Verlag, Berlin 1994.

[7] M.J. Beale, N.G. Chew, M.J. Uren, A.G. Cullis, J.D. Benjamin, *Appl. Phys. Lett.* **46**, 86 (1985).

[8] H.J. von Bardeleben, C. Ortega, A. Grosman, V. Morazzani, J. Siejka, D. Stievenard, Ref. [5], p. 301.

[9] V. Vezin, P. Goudeau, A. Naudon, A. Halimaoui, G. Bomchil, *Appl. Phys. Lett.* **60**, 2625 (1992).

[10] D. Bellet, S. Billat, G. Dolino, M. Ligeon, C. Meyer, F. Muller, *Solid State Comm.* **86**, 51 (1993).

[11] C. Delerue, G. Allan, M. Lannoo, *Phys. Rev. B* **48**, 11024 (1993).

[12] S. Schlupper, S.L. Friedman, M.A. Marcus, D.L. Adler, Y.H. Xie, F.M. Ross, T.D. Harris, W.L. Brown, Y.J. Chabal, L.E. Brus, P.H. Citrin, *Phys. Rev. Lett.* **72**, 2648 (1994).

[13] G. Fishman, I. Mihalcescu, R. Romestain, *Phys. Rev. B* **48**, 1464 (1993).

[14] D.J. DiMaria, J.R. Kirtley, E.J. Pakulis, D.W. Dong, T.S. Kuan, F.L. Pesavento, T.N. Theis, J.A. Cutro, *J. Appl. Phys.* **56**, 401 (1984).

[15] P.A. Badoz, D. Bensahel, G. Bomchil, F. Ferrieu, A. Halimaoui, P. Perret, J.L. Regolini, I. Sagnes, G. Vincent, in: *Microcrystalline Semiconductors — Material Science and Devices*, Eds. P.M. Fauchet, C.C. Tsai, L.T. Canham, I. Shimizu, Y. Aoyagi, in series *Mater. Res. Soc. Symposium Proceedings*, Vol. 283, 1992, p. 97.

[16] G. Vincent, F. Leblanc, I. Sagnes, P.A. Badoz, A. Halimaoui, Ref. [5], p. 217.

[17] J.C. Vial, A. Bsiesy, F. Gaspard, R. Herino, M. Ligeon, F. Muller, R. Romestain, R.M. Macfarlane, *Phys. Rev. B* **45**, 14171 (1992).

[18] I. Mihalcescu, M. Ligeon, F. Muller, R. Romestain, J.C. Vial, Ref. [5], p. 111.

[19] P.D.J. Calcott, K.J. Nash, L.T. Canham, M.J. Kane, D. Brumhead, *J. Phys., Condens. Matter* **5**, L91 (1993).

[20] P.D.J. Calcott, K.J. Nash, L.T. Canham, M.J. Kane, D. Brumhead, Ref. [5], p. 257.

[21] J.C. Vial, A. Bsiesy, G. Fishman, F. Gaspard, R. Herino, M. Ligeon, F. Muller, R. Romestain, Ref. [15], p. 241.

[22] N.O. Lipari, M. Altarelli, *Phys. Rev. B* **15**, 4883 (1977).

[23] R. Romestain, G. Fishman, *Phys. Rev. B* **49**, 1774 (1994).

[24] J.C. Merle, M. Capizzi, P. Fiorini, A. Frova, *Phys. Rev. B* **17**, 4821 (1978).

[25] J.N. Chalzaviel, F. Ozanam, V.M. Dubin, *J. Phys. (Paris) I* **4**, 1325 (1994).

[26] V.M. Dubin, F. Ozanam, J.N. Chalzaviel, unpublished results.

[27] R. Tsu, D. Babic, *Appl. Phys. Lett.* **64**, 1806 (1994).

[28] A. Bsiesy, F. Muller, M. Ligeon, F. Gaspard, R. Herino, R. Romestain, J.C. Vial, *Phys. Rev. Lett.* **71**, 637 (1993).

[29] A. Bsiesy, F. Gaspard, R. Herino, M. Ligeon, F. Muller, R. Romestain, J.C. Vial, unpublished results.

[30] M. Enachescu, E. Hartmann, F. Koch, *Appl. Phys. Lett.* **64**, 1365 (1994).